Synthesis of and Ferromagnetic Coupling in Poly(phenylenevinylene)s Bearing Built-in *t*-Butyl Nitroxides

Hiroyuki Nishide,* Takashi Kaneko, Shuichi Toriu, Yoshihiro Kuzumaki, and Eishun Tsuchida*

Department of Polymer Chemistry, Waseda University, Shinjuku, Tokyo 169

(Received August 21, 1995)

Poly[[2- or 4-[*N*-*t*-butyl-*N*-(triethylsiloxy- or *t*-butyldimethylsiloxy)amino]-1,4- or 1,2-phenylene]vinylene] was synthesized by polymerizing 4- or 2-bromo-2- or 4-[*N*-*t*-butyl-*N*-(triethylsiloxy- or *t*-butyldimethylsiloxy)amino]styrene with a palladium catalyst, respectively. They were deprotected and chemically oxidized to yield poly(1,4- or 1,2-phenylenevinylene)s bearing a 2- or 4-substituted built-in nitroxide radical. The polyradicals were chemically stable, and their spin concentration was increased to 0.8 spin/unit. A SQUID measurement which included the corresponding diradicals and triradicals indicated that a partial, but strong, intramolecular ferromagnetic coupling was established through the conjugated backbone, despite a spin defect in the side radical moiety, for the poly(1,2- phenylenevinylene) bearing 4-substituted built-in nitroxide radical.

Recently, organic molecular-based magnetism has been significantly investigated as one of the undeveloped electronic properties of organic molecules.[1,2] The possibility of high-spin states in π-conjugated organic radicals has been previously discussed,[3—5] and many model compounds of high-spin polyradicals have been proposed on the basis of molecular-orbital theory or valence-bond theory.[6—9] The high-spin state stability of the polyradicals was further discussed in detail based on semiempirical calculations,[10,11] and some accessible polyradicals have been synthesized to date.[12—20] In particular, cross-conjugated polyradicals, such as oligo(phenylenecarbene) and oligo(triarylmethyl), have been experimentally studied and shown to display a multiplet ground state. However, there remains a problem: A small number of spin defects break down π-conjugation in the polymers, or eliminate the magnetic interaction between the spins, because spin generation results in the formation of the cross-conjugated structure, itself.[13,14,21] In addition to this disadvantage, most of these cross-conjugated polyradicals lacked chemical stability at room temperature.

On the other hand, it has been estimated for π-conjugated linear polymers bearing side-chain or pendant radical groups that a spin defect does not break down their π-conjugation system. The radical-pendant type π-conjugated polyradicals possess an advantage over the cross-conjugated polyradicals in that an unavoidable formation of the spin defect accompanying an increase in the degree of polymerization would not influence the expected magnetic interaction through π-conjugation. Although pendant-type polyradicals based on the polyacetylene backbone have been thoroughly investigated from both theoretical[7,8,22] and experimental[16,17,23,24] viewpoints, including our studies, an expected through-bond ferromagnetic interaction could not be observed. We concluded that the through-bond magnetic interaction disappeared due to torsion from the conjugated and presumed planar structures as well as a decrease in spin polarization over the entire macromolecules due to the sterically bulky pendant groups.[18]

We recently reported on the magnetic interaction between chemically stable nitroxide diradicals connected with the stilbene-skeleton **1** on the basis of a semiempirical calculation of the molecular orbital plus the configuration interaction and magnetic measurements.[25] From the viewpoint of the connectivity of stilbene-coupled dinitroxides, the *o*,*m*′- and *m*,*p*′-isomers (*o*,*m*′-**1** and *m*,*p*′-**1**, respectively) displayed a ferromagnetic spin interaction and were selected as dimer units for constructing ferromagnetically coupled polyradicals. Our experimental results concerning the stilbene diradicals also concluded that the head-to-tail linkage of the phenylenevinylene unit was essential for ferromagnetic coupling. That is, the mixture of head-to-tail (*o*,*m*′- or *m*,*p*′-isomers for the stilbene diradicals), head-to-head (*o*,*o*′-isomer for the stilbene diradicals), and tail-to-tail (*m*,*m*′-isomer for the stilbene diradicals) linkage cancels the expected ferromagnetic interaction along the conjugated chain. Thus, the extended polyradicals are poly(1,4- and 1,2-phenylenevinylene)s (1,4- and 1,2-PPV) bearing 2- or 4-substituted built-in nitroxides, as restrictedly represented in *p*- and *o*-**2**, respectively (Chart 1). We have preliminarily reported success in ferromagnetic coupling in poly(phenylenevinylene)s (PPV) bearing the above-mentioned nitroxide[26] and the phenoxy derivative.[27]

In this paper we first describe the syntheses and structures including the restricted head-to-tail linkage of the radical precursor polymers, poly[[2-[*N*-*t*-butyl-*N*-(triethylsiloxy)amino]-1,4-phenylene]vinylene] (*p*-**3a**) and poly[[4-[*N*-*t*-butyl-*N*-(*t*-butyldimethylsiloxy)amino]-1,2-phenylene]vinylene] (*o*-**3b**), from the corresponding bifunctional monomers, 4-bromo-2-[*N*-*t*-butyl-*N*-(triethylsiloxy)amino]-styrene (*p*-**4a**) and 2-bromo-4-[*N*-*t*-butyl-*N*-(*t*-butyldimethylsiloxy)amino]styrene (*o*-**4b**), respectively. The physico-

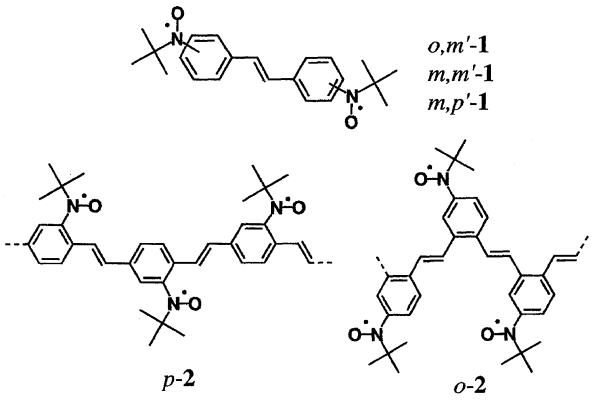

Chart 1.

chemical characteristics of the polyradicals *p*- and *o*-**2**, converted from *p*-**3a** and *o*-**3b** through elimination of the protecting silyl groups, followed by chemical oxidation; also, their ESR and SQUID measurements are described in order to discuss the intramolecular ferromagnetic spin interaction of the nitroxide radicals through the π-conjugated PPV backbone.

Results and Discussion

Synthesis. A mono-substituted PPV involves three linkage structures (head-to-tail, head-to-head, and tail-to-tail) to form the PPV chain. Although PPVs with high molecular weights have usually been synthesized via sulfonium precursor polymers,[28,29] they lack the restricted primary structure of head-to-tail, because the polymerization proceeds through a repeated elimination reaction of the dialkyl sulfide from α,α′-bis(dialkylsulfonio) xylenes. We attempted and compared the synthesis of the head-to-tail linked PPVs via the Wittig reaction[30] of (formylphenyl)methyl phosphonium salts and the Heck reaction[31,32] of bromostyrene derivatives using a palladium catalyst. The Heck reaction was more favorable than the Wittig reaction to yield PPVs with a relatively high molecular weight and an all *trans*-vinylene structure.

Monomers *p*- and *o*-**4** for polymerization via the Heck reaction were synthesized according to Scheme 1. Bromoiodostyrene was prepared from bromoiodotoluene according to a previous report.[33] The *t*-butylhydroxyamino group was introduced by lithiation of iodobromostyrene followed by the addition of 2-methyl-2-nitrosopropane according to a method of Forrester.[34] The coupling reaction of bromoiodostyrene preferentially proceeded at the iodo position because the reactivity of the iodo group during lithiation is much higher than that of the bromo group. The triethylsilyl and *t*-butyldimethylsilyl groups were used to protect the hydroxyl group,[35] because they were sufficiently stable compared with the trimethylsilyl group under the following basic conditions during the polymerization.

Monomers *p*- and *o*-**4** were polymerized via the Heck reaction using palladium acetate as the catalyst. Tri-*o*-tolylphosphine and triethylamine were also added as a co-catalyst or the ligand of Pd and as a base for the eliminated HBr, respectively. The molar ratio [Pd]/[monomer] was 1/10 in the feed, DMF served as the polymerization solvent, and the polymerization temperature was 100 °C in order to promote polymerization and to avoid side reactions, such as crosslinking (Table 1). The polymerization of *p*-**4c** hardly proceeded, suggesting a poisoning effect of the hydroxyamino group against the Pd catalyst. The monomers, *p*-**4a**, **b** and *o*-**4a**, **b**, whose hydroxyamino groups were protected with trialkylsilyl groups, were polymerized to yield the corresponding polymers, *p*-**3a**, **b** and *o*-**3a**, **b**, respectively (Scheme 2), with satisfactory yields and molecular weights. The degree of polymerization of these polymers, measured by GPC, coincided with those determined by terminal bromine analysis. The relatively low yields and molecular weights for *p*-**3a** and **b** would be explained by a steric hindrance of the *o*-substituent neighboring the reacting vinyl group. The polymers, *p*-**3a**, **b** and *o*-**3a**, **b**, were a yellowish powder which was soluble in DMF, $CHCl_3$, benzene, THF, and acetone, but insoluble in alcohols and aliphatic hydrocarbons.

Table 1. Examples of Polymerization of the Bromostyrene Derivatives **4**

Monomer	Time/h	Yield/%	$\overline{M}_w/10^3$	$\overline{M}_w/\overline{M}_n$
p-**4a**	24	48	3.5	2.0
p-**4b**	24	22	3.4	1.2
p-**4c**	24	3	1.7	1.5
o-**4a**	6	25	5.8	1.1
o-**4b**	6	26	6.5	2.0
	6	60	2.7	1.5

$[Monomer]_0$ = 0.3 M, $[Pd(OAc)_2]/[Monomer]_0$ = 1/10, $[P(C_6H_4CH_3)_3]/[Pd(OAc)_2]$ = 2, [triethylamine]/$[Monomer]_0$ = 2.5—5, temp 100 °C.

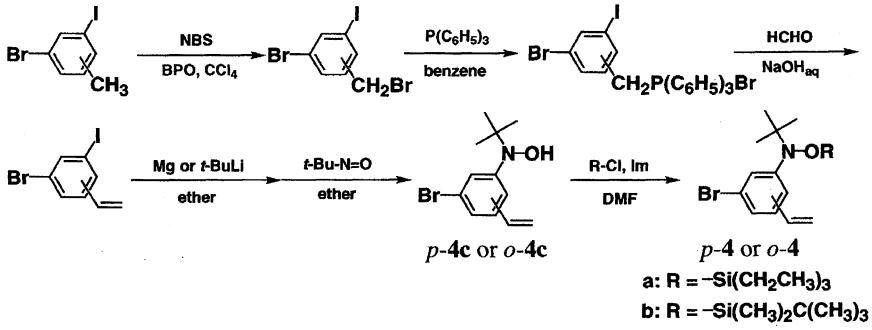

Scheme 1.

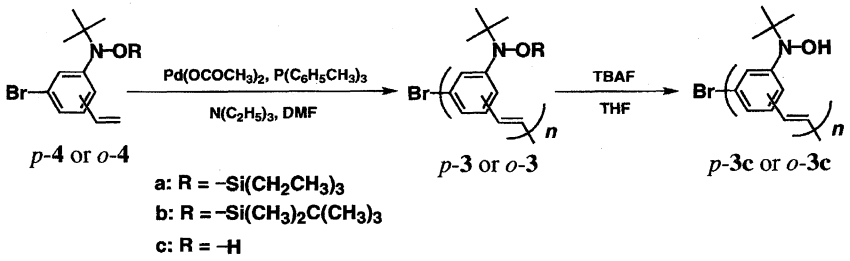

Scheme 2.

The polymers, *p*-**3a**, **b** and *o*-**3b**, showed IR absorption attributed to an out-of-plane bending mode of the *trans*-vinylene at 960—970 cm^{-1}. The fluorescence at 485 and 510 nm, and 475 nm (λ_{ex} 420 nm) of *p*-**3a** and *o*-**3b**, respectively, was ascribed to the *trans*-vinylene structure. The ^{13}C NMR of *o*-**3b** gave 8 lines, ascribed to the carbons of the phenyl ring and the vinylene bond. These supported the head-to-tail and *trans*-vinylene linkage structure in the 1,4- and 1,2-PPV skeleton, which was synthesized via a Heck reaction of the bromostyrene derivatives.

The polymers, *p*-**3a**, **b** and *o*-**3a**, **b**, were converted to *p*- and *o*-**3c**, respectively, after eliminating the protecting silyl group with tetrabutylammonium fluoride (TBAF) in a THF solution. The thorough disappearance of the absorption $\nu_{Si-C} = 1230\ cm^{-1}$ and the appearance of $\nu_{O-H} = 3443\ cm^{-1}$ in the IR spectrum of *p*-**3a** supported a complete elimination of the protecting silyl group and the formation of *p*-**3c**. However, elimination of the silyl group was not completed for *p*-**3b**, probably due to the bulky substituent in the *o*-position of the backbone. In the following experiment, *p*-**3a** was employed to give the polyradical *p*-**2**. The complete elimination of the trialkylsilyl group was confirmed for both *o*-**3a** and **b**, while the elimination of *o*-**3a** partially proceeded even under basic polymerization conditions; *o*-**3b** was employed to give the following polyradical *o*-**2**. The solvent solubility was significantly reduced in the hydroxyamino polymers, *p*- and *o*-**3c**, which resulted from a hydrogen-bond interaction between the hydroxyamino groups.

Polyradicals *p*- and *o*-**2** were obtained by a treatment of *p*-**3a** and *o*-**3b** in THF with TBAF and fresh PbO_2. The spin concentrations were determined by doubly integrating the ESR signals with 2,2,6,6-tetramethyl-1-piperidinyloxyl (TEMPO) solutions as a standard. The spin concentration of *o*-**2** reached ca. 4.8×10^{23} spins/unit mol (0.8 spin/unit) by selecting the oxidative conditions. However, the oxidation of *p*-**3** could not bring about a high spin concentration; in *p*-**2**, a side reaction, such as intramolecular oxygen migration, might occur between the *t*-butyl nitroxide residue and the neighboring vinylene group. On the other hand, *o*-**2** was extremely stable and maintained the initial spin concentration under the conditions of the following ESR and SQUID measurements.

Several oligomer radicals were also synthesized as references of the polyradicals. 1-[3-(*N*-*t*-Butylhydroxyamino)styryl]-4-[4-(*N*-*t*-butylhydroxyamino)styryl]benzene (**5b**) and 1-[3-(*N*-*t*-butylhydroxyamino)styryl]-2-[4-(*N*-*t*-butylhydroxyamino)styryl]benzene (**6b**) were synthesized by the Heck reaction using the reaction selectivity of the iodo position to bis(bromostyryl)benzene, followed by a coupling reaction with 2-methyl-2-nitrosopropane to introduce the *t*-butylhydroxyamino substituent (Chart 2). 1,2-Distyryl-4-[*N*-*t*-butyl-*N*-(*t*-butyldimethylsiloxy)amino]benzene (**7a**) and 2,2′-distyryl-4,5′-bis[*N*-*t*-butyl-*N*-(*t*-butyldimethylsiloxy)amino]stilbene (**8a**) were synthesized by the Heck reaction from a mixture of monomer **4b** with bromobenzene and styrene, and then purified by HPLC. These hydroxylamines, **5b** and **6b**, were treated with Ag_2O or PbO_2 in a degassed benzene solution to give the corresponding radicals, **5c** and **6c**, respectively. The radicals, **7c** and **8c**, were prepared from **7a** and **8a**, respectively, by using the same procedure as the polyradicals.

Spectral Analysis. The UV-vis spectra of *p*-**3** showed an absorption maximum (λ_{max}) at 400—410 nm (DMF, $\varepsilon = 8.8\times10^3\ dm^3\ cm^{-1}$ monomer unit mol^{-1}), suggesting a developed π-conjugation compared with the previously reported λ_{max} (355—378 nm) for oligo(1,4-phenylenevinylene).[36] The λ_{max} (400 nm) of the cast film of the hexyloxy-substituted 1,4-PPV, which was synthesized by the Heck reaction and was previously reported by us,[37] almost agreed with that of the unsubstituted 1,4-PPV, which was synthesized from a sulfonium salt precursor polymer, and was well-characterized as a significantly π-conjugated polymer.[38] This supports the developed π-conjugation in the 1,4-PPV backbone, even after introducing a bulky substituent group into the backbone. On the other hand, UV-vis absorption with λ_{max} at 309 nm and extended to 360 nm for *o*-**3b** suggested an undeveloped π-conjugation compared with *p*-**3a**. Such insufficiently extended absorption was also observed for the unsubstituted and hexyloxy-substituted 1,2-PPV, which would

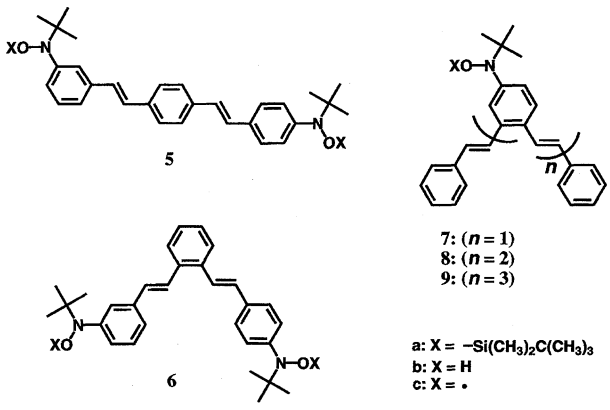

Chart 2.

be ascribed to the nature of the 1,2-PPV backbone. The UV-vis absorption maxima of the 1,4-PPV derivatives and shoulder absorption of the 1,2-PPV derivatives are plotted in Fig. 1. With the degree of polymerization, the λ_{max} of 1,4-PPV, and even the shoulder absorption of 1,2-PPV, shifted to longer wavelengths, which corresponded to the development of π-conjugation. These λ_{max} (or $\lambda_{shoulder}$) shifts agreed with the λ_{max} (or $\lambda_{shoulder}$) calculated by a semiempirical method (PPP[39]).

The ionization thresholds (I^{th}) of *p*-**3a** and *o*-**3b** were estimated in our previous study[37] by ultraviolet photoelectron spectroscopy to be 5.7 and 5.9 eV, respectively. This agrees with the above estimation from the UV-vis absorption spectra, and suggests a more developed π-conjugation for *p*-**3a**. Although I^{th} slightly increased from *p*-**3a** to *p*-**2** (5.8 eV), it decreased from *o*-**3b** to *o*-**2** (5.5 eV) after conversion to the polyradicals.[37] These I^{th} values of the polyradicals could be assigned to the conjugated PPV backbone, because the I^{th} values of the nitroxide radicals were 7—10 eV, estimated from calculations and/or experiments.[40,41] The changes in I^{th} through the chemical oxidation of the pendant groups in *p*-**3a** and *o*-**3b** to the radicals were considered to be caused by the nitroxide substituent group and/or a structural transformation to $=N^+-O^-$ through electron migration from the N–O group to the phenyl ring. However, the slight increase or decrease in the π-conjugation of the PPV backbone was not significant for the following magnetic study.

The ESR spectrum of *p*-**2** at a low spin concentration gives a three-line signal at $g=2.006$, ascribed to hyperfine coupling with a nitrogen nucleus (Fig. 2a). The hyperfine coupling constant ($a_N = 1.39$ mT) coincided with the previously reported $a_N = 1.42$ mT[25] for *t*-butyl (*o*-styrylphenyl) nitroxide. This indicates a localization of the unpaired electron over almost the N–O group, which is induced by the large dihedral angle between the N–O bond and the phenyl plane due

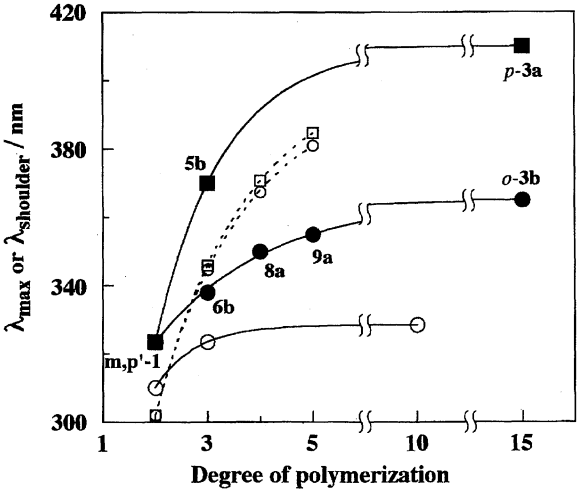

Fig. 1. UV/vis absorption vs. degree of polymerization for the *p*- (■) and *o*-**3** (●) derivatives, for stilbene, distyrylbenzene and the unsubstituted 1,2-PPV (○), and for the semiempirical calculation (PPP) values (dashed lines) of 1, 4- (□) and 1,2-PPV (○).

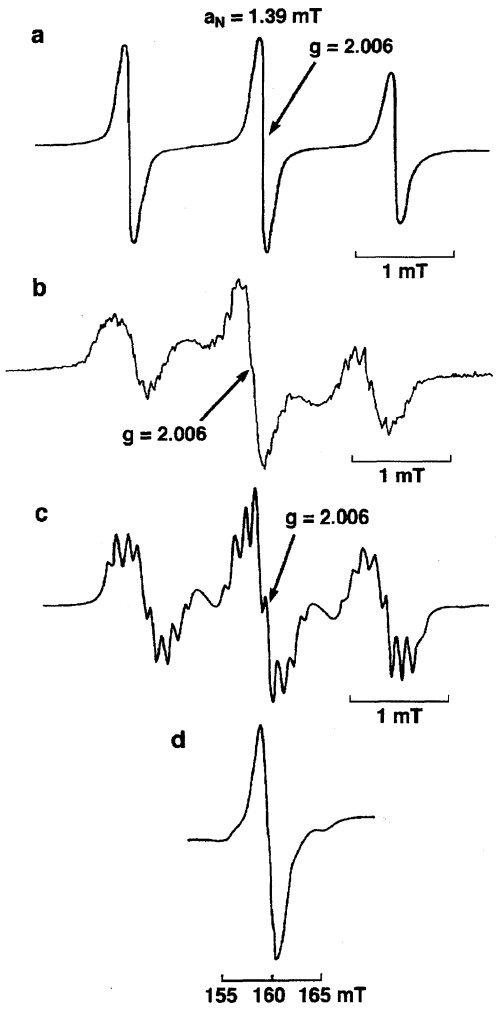

Fig. 2. ESR spectra of the polyradicals. (a) *p*-**2** in benzene: polymer concn 1 unit mM (spin concn 0.01 spin/unit), (b) *o*-**2** in THF: polymer concn 1 unit mM (spin concn 0.25 spin/unit), (c) **7c** in THF at 1 mM, (d) *o*-**2** in 2-methyltetrahydrofuran (spin concn 0.38 spin/unit) at 5.5 K.

to a steric interference of the bulky *t*-butyl nitroxide residue substituted in the *o*-position of the backbone.

The ESR spectrum of *o*-**2** at a low spin concentration shows not only the hyperfine coupling at $g=2.006$, ascribed to a nitrogen nucleus, but also a multiplet attributed to the backbone phenylene protons (Fig. 2b). It was difficult to analyze the spectrum, probably due to the effect of anisotropic and/or exchange broadening of the nitroxide fixed along the backbone; however, the hyperfine coupling constant ascribed to the nitrogen nucleus ($a_N = 1.2$ mT) agreed with the values of *t*-butyl (*m*- and *p*-styrylphenyl) nitroxide ($a_N = 1.26$[25] and 1.14 mT,[42] respectively). Since *t*-butyl (*m*- and *p*-styrylphenyl) nitroxide gave the quantitative hyperfine coupling constant (0.013[25] and 0.11 mT,[42] respectively) attributed to the vinylene protons, *o*-**2** is presumed to also possess a high spin density distribution through the vinylene moiety.

The above discussion was supported by the corresponding monoradical substituted trimer **7c**, which represented the partial molecular structure of *o*-**2**. The ESR spectrum of

7c is similar to that of *o*-**2** at low spin concentration (Fig. 2c), while the proton hyperfine structure is more clearly observed for **7c**.[43] We carefully carried out a simulation of the ESR spectrum given in Fig. 2c;[44] the $a_N = 1.15$ mT determined by this simulation was almost suited to that of *t*-butyl (*p*-styrylphenyl) nitroxide. The a_H values of 0.02 and 0.12 mT, attributed to the vinylene protons, corresponded to the reported values for *t*-butyl (*m*- and *p*-styrylphenyl) nitroxides,[25,42] respectively. A delocalized spin distribution into the phenylene ring of the PPV backbone is postulated for *o*-**2**, because the *t*-butyl nitroxide moiety substituted in the *m*-position of the PPV backbone is not twisted to the phenylene ring, compared with *p*-**2**, which suffers a steric hindrance at the *o*-substitution.

The ESR spectrum of *o*-**2** changed to broad signals with increasing spin concentration, due to a locally high spin concentration along the polymer backbone. Although no fine structure to give zero-field splitting parameters *D* or *E*[45] was detected, the $\Delta m_s = \pm 2$ forbidden transition ascribed to the triplet species was observed at $g = 4$ in frozen 2-methyltetrahydrofuran glass (Fig. 2d). The ESR signal in the $\Delta m_s = \pm 2$ region was doubly integrated to give Curie plots. The signal intensity of *o*-**2** was essentially proportional to the reciprocal of the absolute temperature in the region of 5.5—70 K.

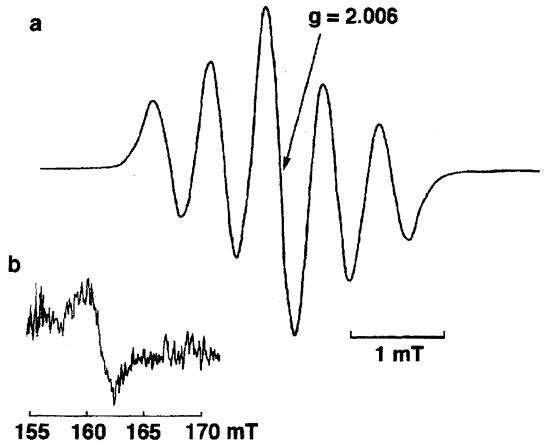

Fig. 3. ESR spectra of **6c** (a) at room temperature and (b) at 77 K in toluene glass.

The ESR spectra of **5c** and **6c** at room temperature showed a five-line hyperfine structure at $g = 2.006$ with a relative signal intensity of 1 : 2 : 3 : 2 : 1, attributed to the coupling of two nitrogen nuclei with the two unpaired electrons (Fig. 3a). The $\Delta m_s = \pm 2$ transitions for the triplet species were also clearly observed at $g = 4$ in frozen toluene glass at 77 K (Fig. 3b). This indicated that the spin-exchange coupling is maintained at $J \gg a_N$ =ca. 1.3 mT in spite of the non-radical phenylene-vinylene spacing unit between the two radical units.

Magnetic Properties. The static magnetic susceptibility of *o*-**2** in a powder sample nearly followed the Curie–Weiss law ($\chi = C/(T - \theta_w)$) (Fig. 4). The Curie constant (C) and Weiss temperature (θ_w), estimated by a linear fitting to $1/\chi$ vs. T plots at 50—290 K, were 7.3×10^{-4} emu K g^{-1} and 1.8 K, respectively. The Curie–Weiss plots were reversible during temperature depressing and elevating, which indicated the chemical stability of the polyradical *o*-**2**. The Curie constant gave a spin concentration for the polyradical (e.g. 0.38 spin/unit in Fig. 4 for *o*-**2**).

The relationship of $\chi_{mol}T$ vs. T is appropriate for studying the spin coupling for an anisotropic or low-dimensional spin coupling, where χ_{mol} is the molar paramagnetic susceptibility. In Fig. 4, the $\chi_{mol}T$ value of *o*-**2** significantly decreases at low temperature, indicating an antiferromagnetic interaction. However, the plots at 50—150 K slightly deviate upward from the theoretical value, $\chi_{mol}T = 0.375$ emu K mol^{-1} for $S = 1/2$, which indicates a ferromagnetic behavior of *o*-**2**.

Figure 5 shows $\chi_{mol}T$ vs. T plots for *o*-**2** diluted in diamagnetic 2-methyltetrahydrofuran to minimize any intermolecular magnetic interactions. An antiferromagnetic interaction observed in a powder sample of *o*-**2** at low temperature is much diminished, and an upward deviation at high temperature is more clearly observed. The magnetic property of *o*-**2** involves both a ferromagnetic interaction through the intramolecular π-electron system and an antiferromagnetic intermolecular (through-space) interaction.

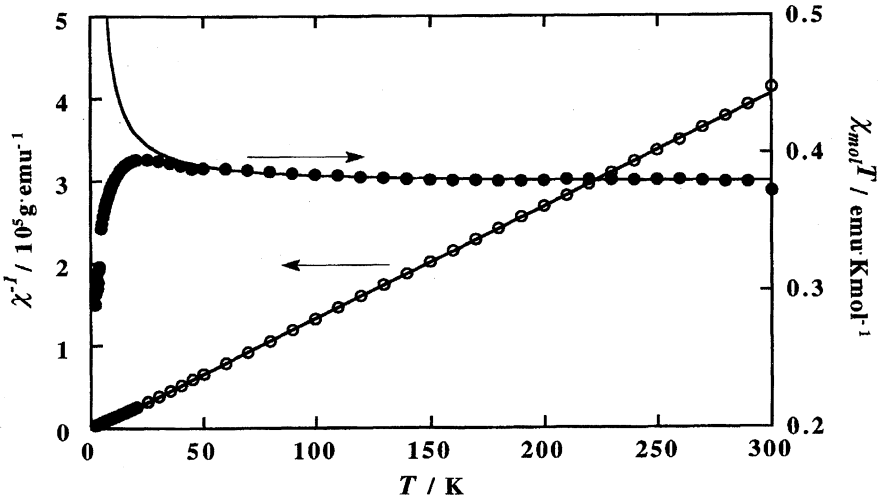

Fig. 4. χ^{-1} vs. T (○) with the Curie–Weiss fit (solid line) and $\chi_{mol}T$ vs. T plots (●) of the powder *o*-**2** at spin concn 0.38 spin/unit.

The magnetization (M), normalized by the saturated magnetization (M_s), M/M_s, is represented by the following Brillouin function ($B(a)$) (Eq. 1):[45]

$$\frac{M}{M_s} = B(a) = \frac{2S+1}{2S}\coth\left(\frac{2S+1}{2S}a\right) - \frac{1}{2S}\coth\left(\frac{a}{2S}\right)$$
$$\text{and } a = \frac{gS\mu_B H}{kT}. \quad (1)$$

The M/M_s of *o*-**2** is plotted versus the effective temperature ($T-\theta$), and compared with the Brillouin curves (Fig. 6). The θ is a coefficient of the weak (antiferro)magnetic interaction between radicals, corresponding to the Weiss temperature of the Curie–Weiss law, and is determined from curve fitting using the following $\chi_{mol}T$ data. The M/M_s plots of *o*-**2** in a 0.5—7 T magnetic field locate between the theoretical Brillouin curves for $S=1/2$ and $S=2/2$ at 2—10 K, and are almost on the curve of $S=2/2$ at 10 K, indicating a ground-state high-spin multiplicity.

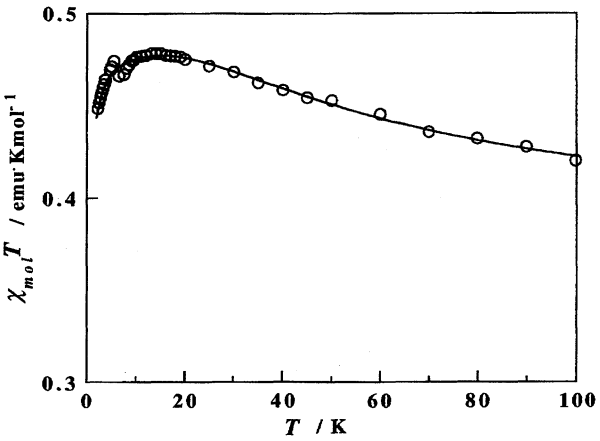

Fig. 5. $\chi_{mol}T$ vs. T plots (●) of the *o*-**2** in frozen 2-methyltetrahydrofuran at spin concn 0.54 spin/unit. Solid line is the theoretical curve calculated with Eq. 9 for $2J=67$ cm^{-1}, $2J'=3$ cm^{-1}, $\theta=-0.31$ K, $x_1=0.07$, $x_2=0.76$, $x_3=0.17$ and $y=0.32$.

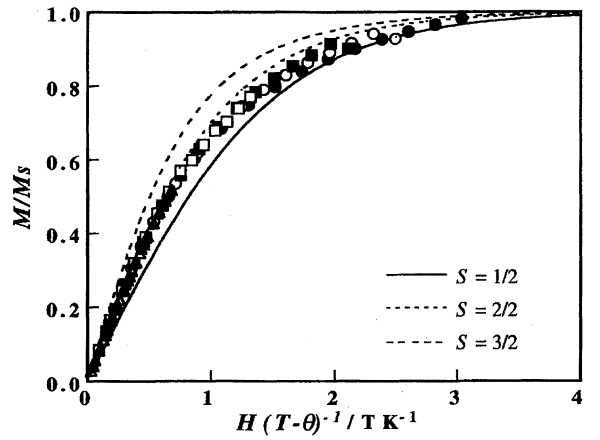

Fig. 6. Normalized plots of magnetization (M/M_s) vs. the ratio of magnetic field and temperature ($H/(T-\theta)$) for *o*-**2** with spin concn 0.54 spin/unit in 2-methyltetrahydrofuran glass at T=2 (●), 2.5 (○), 3 (■), 5 (□), 10 (▲), 15 (△) K and the theoretical curves corresponding to the $S=1/2$, 1, and 3/2 Brillouin functions, where θ is weak antiferromagnetic term and was determined to be -0.31 K from the $\chi_{mol}T$ vs. T plots.

The magnetization and magnetic susceptibility of the diradicals, **8c** and **6c**, were measured in order to estimate the intramolecular spin coupling in *o*-**2**; **8c** and **6c** are model compounds that determine the spin coupling between the neighboring units and the next neighboring units, respectively. 2-Methyltetrahydrofuran was used as a diluent of the diradicals to minimize intermolecular interactions. The M/M_s plots of **8c** and **6c** were also presented between the Brillouin curves for $S=1/2$ and $S=1$ at 2—10 K. The μ_{eff}/μ_B values of **8c** and **6c** were reduced by the spin concentrations of 1.00 and 1.22 spin/molecule, respectively, which were determined by carefully integrating the ESR signals compared with those of a TEMPO solution as the standard, and by the saturated magnetization at 2 K, and are given in Fig. 7. μ_{eff}/μ_B plots of **8c** and **6c** locate at the intermediate between $\mu_{eff}/\mu_B=2.45$ and 2.83 for $S=1/2$ and 1, respectively.

Magnetic susceptibility (χ) is defined as

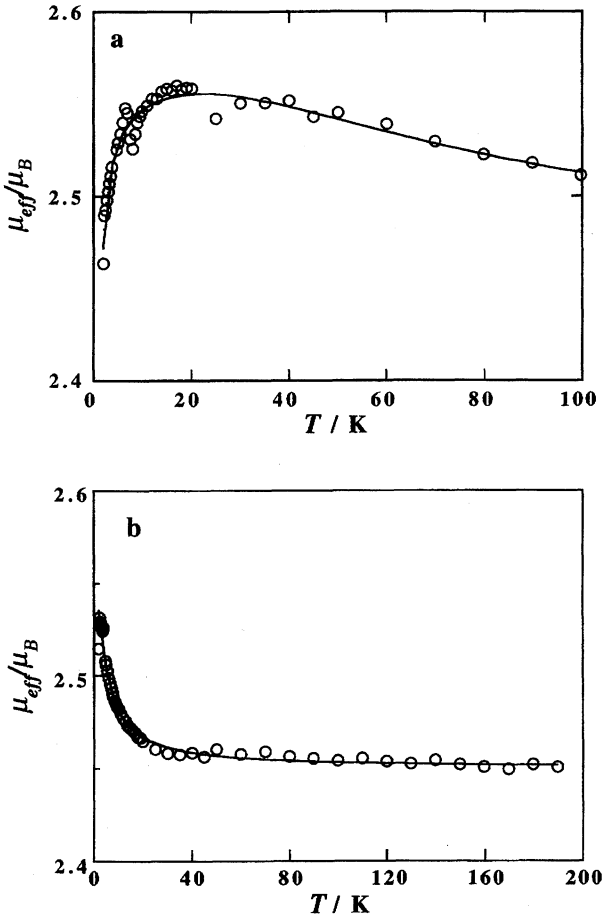

Fig. 7. μ_{eff}/μ_B vs. T plots (a) of **8c** at spin concn 1.00 spin/molecule and (b) of **6c** at spin concn 1.21 spin/molecule. Solid lines are the theoretical curves calculated with Eq. 6 with $2J=67$ cm^{-1}, $\theta=-0.16$ K, and $x=0.71$ for (a), and with $2J=3$ cm^{-1}, $\theta=-0.06$ K, and $x=0.61$ for (b).

$$\chi = \frac{N_u \mu_{eff}^2}{3kT}, \quad (2)$$

where N_u is the average molecular number measured ($N_u = N_s/L$ where N_s and L are the spin number measured and the spin site number formulated in one molecule, respectively; in the case of **6c**, L=2.). The μ_{eff}/μ_B is proportional to $(\chi T)^{1/2}$,

$$\frac{\mu_{eff}}{\mu_B} = \left(\frac{3k}{N_u \mu_B^2}\chi T\right)^{1/2}. \quad (3)$$

The spin-exchange interaction in a two-spin system (Fig. 8a) is expressed by the Heisenberg Hamiltonian,[46]

$$\mathcal{H} = -2J\boldsymbol{S}_1 \cdot \boldsymbol{S}_2, \quad (4)$$

where J is the spin-exchange coupling constant. Equation 4 is converted to the following equation based on a consideration of the relative thermally induced populations of the states of different spin,[47] which is the well-known Bleaney–Bowers expression,[48]

$$\chi = \frac{2N_d g^2 \mu_B^2}{k(T-\theta)(3+\exp(-2J/kT))}. \quad (5)$$

The magnetic susceptibility of a diradical sample with incomplete radical generation, such as **8c**, is expressed by the sum of the diradical fraction (Eq. 5) and the impurity fraction of the monoradical ($\chi = N_m g^2 \mu_B^2/4k(T-\theta)$); also, Eq. 3 is modified to Eq. 6. Here, N_d and N_m are the molecular number of the diradical fraction and that of the monoradical, respectively, and $N_s = 2N_d + N_m = 2N_u$.

$$\mu_{eff}/\mu_B = \left(\frac{6g^2T}{(T-\theta)(3+\exp(-2J/kT))}(1-x_1) + \frac{3g^2T}{2(T-\theta)}x_1\right)^{1/2}, \quad (6)$$

where θ and x_1 is the Weiss constant for a weak intermolecular magnetic interaction and the fraction of the doublet or monoradical species in the total spin number ($x_1 = N_m/N_s$), respectively.

Curve fitting of the μ_{eff}/μ_B data for **8c** to Eq. 6 gave $2J = 67 \pm 11$ cm^{-1}, $\theta = -0.16 \pm 0.01$ K and $x_1 = 0.71 \pm 0.06$; that for **6c** gave $2J = 3 \pm 2$ cm^{-1}, $\theta = -0.06 \pm 0.16$ K and $x_1 = 0.6 \pm 0.4$. The positive $2J$ value indicates the expected through-bond intramolecular ferromagnetic exchange coupling of **8c** and **6c**. The $2J$ of **8c** is ca. 1.5-times larger than $2J$=41 cm^{-1} of the corresponding simple dimer model *m,p'*-**1** previously reported by us.[25] It is considered that the triplet state of **8c** is stabilized by both the end-capped and conjugated phenyl groups or the decrease in the potential energy gap between two NBMOs caused by the developed π-conjugation; the latter was supported by the above-mentioned UV/vis absorption maxima. This consideration is in accordance with a semiempirical calculation.[49]

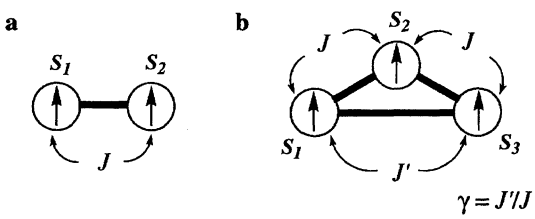

Fig. 8. Spin-exchange coupling structure of (a) a two spin system and (b) a isoscelestriangular three spin system.

The $2J$ of **6c** is reduced to ca. 1/10 (from *m,p'*-**1** to **6c**) in response to the conjugated, but spacing phenylenevinylene, unit. This reduction is almost consistent with the spacing phenylenevinylene effect estimated by a semiempirical calculation.[49] In any case, it is concluded that a ferromagnetic interaction is established through the conjugated PPV backbone, even in the presence of a spin defect for polyradical *o*-**2**.

The spin-exchange interaction in an isoscelestriangular three spin system (Fig. 8b) is expressed by the spin Hamiltonian,[50]

$$\mathcal{H} = -2J(\boldsymbol{S}_1 \cdot \boldsymbol{S}_2 + \boldsymbol{S}_2 \cdot \boldsymbol{S}_3 + \gamma \boldsymbol{S}_3 \cdot \boldsymbol{S}_1), \quad (7)$$

where J is the spin-exchange coupling constant. Equation 7 is solved in the same way as Eq. 4 to give

$$\chi = \frac{N_t g^2 \mu_B^2}{4k(T-\theta)} \cdot \frac{10+\exp(-(1+2\gamma)J/kT)+\exp(-3J/kT)}{2+\exp(-(1+2\gamma)J/kT)+\exp(-3J/kT)}, \quad (8)$$

where $\gamma = J'/J$ is defined, and the equation is the same as that of a linear three-spin system when $\gamma = 0$. The spin-exchange interaction for *o*-**2** closely resembles the sum of a three-, two-, and one-spin system, because the average spin quantum number(s) of *o*-**2** appears to be $S < 3/2$ in Fig. 6. Therefore, the $\chi_{mol}T$ of *o*-**2** is expressed as

$$\chi_{mol}T = \frac{N_A g^2 \mu_B^2 T}{k(T-\theta)} \left(\frac{x_3}{12} \cdot \frac{10+\exp(-(J+2J')/kT)+\exp(-3J/kT)}{2+\exp(-(J+2J')/kT)+\exp(-3J/kT)} + \frac{x_2(1-y)}{3+\exp(-2J/kT)} + \frac{x_2 y}{3+\exp(-2J'/kT)} + \frac{x_1}{4}\right), \quad (9)$$

Here, N_t, N_d, and N_m are the molecular number of the triradical, diradical, and monoradical fraction, respectively, and $N_s = 3N_t + 2N_d + N_m = 3N_u$, $x_1 = N_m/N_s$, $x_2 = 2N_d/N_s$ and $x_3 = 3N_t/N_s$. Here, y is the ratio of the diradical fraction with the spin-exchange coupling constant (J'). $2J$=67 cm^{-1} and $2J'$=3 cm^{-1} from the curve fitting of **8c** and **6c**, and $x_1 = 0.07$ were substituted in Eq. 9, which was fitted to the experimental $\chi_{mol}T$ data of *o*-**2**. The best-fit (correlation coefficient R=0.97) parameters were $y = 0.3 \pm 0.1$, $x_3 = 0.17 \pm 0.04$, $\theta = -0.31 \pm 0.05$. The actual spin-exchange coupling constant between the radicals in *o*-**2** almost agreed with those in the diradicals, which also did not conflict with the result estimated for a linear three-spin system ($\gamma = 0$).

Conclusion

Poly(1,2-phenylenevinylene) bearing a 4-substituent nitroxide *o*-**2**, even with a spin concentration of 0.54, revealed an S value of ca. 2/2, indicating a high-spin ground state

in the polyradical. The experimental spin coupling constant, $2J$=67 and 3 cm^{-1}, for the diradical model compound **8c** and the diradical involving one spacing phenylenevinylene unit **6c**, respectively, were effective in the Eq. 9 expression for a three-spin system to reproduce the ferromagnetic behavior in $\chi_{mol}T$ of the polyradical *o*-**2**.

Experimental

Bromoiodostyrene. Bromoiodotoluene (59 g, 0.20 mol), which was prepared from the corresponding nitroaminotoluene, was dissolved in 680 ml of tetrachloromethane. After *N*-bromosuccinimide (36 g, 0.20 mol) and benzoyl peroxide (0.4 g, 2 mmol) were added to the solution, the mixture was refluxed for 3 h. Then after cooling, the mixture was filtered, and the filtrate was evaporated and dissolved in 800 ml of benzene. Triphenylphosphine (52 g, 0.20 mol) was added to the solution and stirred for 1 h at 70 °C to yield a white precipitate of the phosphonium salt. The precipitate was filtered and washed with ether to yield 84 g of [(bromoiodophenyl)methyl]triphenylphosphonium bromide (yield 66%). The phosphonium salt (77 g, 0.12 mol) was suspended in 960 ml of 25% formalin; 220 ml of 5 M-sodium hydroxide (M=mol dm^{-3}) was then added dropwise to the mixture over a period of 20 min. The mixture was stirred for 1 h at room temperature and extracted with ether. The extract was washed with water and dried over anhydrous sodium sulfate. The crude product was separated by silica-gel chromatography with hexane/chloroform (1/1) eluent to yield bromoiodostyrene.

4-Bromo-2-iodostyrene: Yield 59%; IR (KBr pellet) 1624 cm^{-1} (νHC=CH_2); ^{1}H NMR ($CDCl_3$, 90 MHz) δ=5.33 (d, 1H, J=11 Hz, –CH=C**H**$_2$), 5.62 (d, 1H, J=17 Hz, –CH=C**H**$_2$), 6.80 (dd, 1H, J=11, 17 Hz, –C**H**=CH_2), 7.35 (d, 1H, J=8 Hz, Ph), 7.45 (d, 1H, J=8 Hz, ArH), 7.97 (s, 1H, ArH); MS *m/z* 310 (M^++2), 308 (M^+).

2-Bromo-4-iodostyrene: Yield 84%; IR (KBr pellet) 1624 cm^{-1} (νHC=CH_2); ^{1}H NMR ($CDCl_3$, 60 MHz) δ=5.9 (d, 1H, J=11 Hz, –CH=C**H**$_2$), 6.2 (d, 1H, J=17 Hz, –CH=C**H**$_2$), 7.4 (dd, 1H, J=11, 17 Hz, –C**H**=CH_2), 7.7 (d, 1H, J=8 Hz, ArH), 8.1 (d, 1H, J=8 Hz, ArH), 8.4 (s, 1H, ArH); MS *m/z* 310 (M^++2), 308 (M^+).

Bromo(*N*-*t*-butylhydroxyamino)styrene. A pentane solution (60 ml) of *t*-butyllithium (96 mmol) was added to bromoiodostyrene (25 g, 80 mmol) in 120 ml of ether at −70 °C. After the solution had been stirred for 0.5 h at −70 °C, 2-methyl-2-nitrosopropane (10 g, 120 mmol) in 120 ml of ether was added, then stirred for 1 h at room temperature. The solution was first washed with aqueous ammonium chloride and then with water. The ether layer was dried over anhydrous sodium sulfate. After evaporation, the crude product was purified by column chromatography on silica gel (chloroform/hexane) to give the bromo(*N*-*t*-butylhydroxyamino)styrene derivative as white crystals.

4-Bromo-2-(*N*-*t*-butylhydroxyamino)styrene (*p*-4c): Yield 18%; mp 92—94 °C; IR (KBr pellet) 3225 (νO–H), 2890—2925 (νalkyl), 1630 cm^{-1} (νHC=CH_2); ^{1}H NMR ($CDCl_3$, 90 MHz) δ= 1.10 (s, 9H, *t*-butyl), 5.18 (d, 1H, J=11 Hz, –CH=C**H**$_2$), 5.58 (d, 1H, J=19 Hz, –CH=C**H**$_2$), 5.74 (s, 1H, OH), 7.08 (dd, 1H, J=11, 19 Hz, –C**H**=CH_2), 7.26 (d, 1H, J=8 Hz, ArH), 7.30 (d, 1H, J=8 Hz, ArH), 7.70 (s, 1H, ArH). Found: C, 53.2; H, 5.9; N, 5.1%. Calcd. for $C_{12}H_{16}BrNO$: C, 53.3; H, 5.9; N, 5.2%.

2-Bromo-4-(*N*-*t*-butylhydroxyamino)styrene (*o*-4c): Yield 35%; mp 70—72 °C; IR (KBr pellet) 3229 (νO–H), 2934—2976 (νalkyl), 1626 cm^{-1} (νHC=CH_2); ^{1}H NMR ($CDCl_3$, 270 MHz) δ=1.09 (s, 9H, *t*-butyl), 5.27 (d, 1H, J=11 Hz, –CH=C**H**$_2$), 5.61 (d, 1H, J=17 Hz, –CH=C**H**$_2$), 6.95 (dd, 1H, J=11, 17 Hz, –C**H**=CH_2), 7.03 (dd, 1H, J=2, 8 Hz, ArH), 7.33 (d, 1H, J=8 Hz, ArH), 7.36 (d, 1H, J=2 Hz, ArH); ^{13}C NMR ($CDCl_3$) δ=25.73, 60.99, 115.79, 122.30, 123.67, 125.10, 128.39, 134.03, 135.18, 149.31; MS *m/z* 271 (M^++2), 269 (M^+).

Bromo[*N*-*t*-butyl-*N*-(trialkylsiloxy)amino]styrene. Bromo(*N*-*t*-butylhydroxyamino)styrene (5.4 g, 20 mmol), trialkylsilyl chloride (6.0 g, 40 mmol), and imidazole (6.8 g, 100 mmol) were dissolved in 36 ml of DMF, and stirred for 12—24 h at 60 °C. The reaction mixture was extracted with hexane and then washed with water. The hexane layer was dried over anhydrous sodium sulfate. After evaporation, the crude product was purified by column chromatography on silica gel (chloroform/hexane) to give bromo-[*N*-*t*-butyl-*N*-(trialkylsiloxy)amino]styrene.

4-Bromo-2-[*N*-*t*-butyl-*N*-(triethylsiloxy)amino]styrene (*p*-4a): Yield 44%; IR (NaCl) 3070 (νC–H(Ar)), 2900—2970 (νC–H(Alkyl)), 1630 cm^{-1} (νC=C); ^{1}H NMR ($CDCl_3$, 90 MHz) δ=0.5 (q, 6H, J=8 Hz, Si–C**H**$_2$CH$_3$), 0.8 (t, 9H, J=8 Hz, Si–CH$_2$C**H**$_3$), 1.1 (s, 9H, *N*-*t*-butyl), 5.18 (d, 1H, J=11 Hz, –CH=C**H**$_2$), 5.61 (d, 1H, J=18 Hz, –CH=C**H**$_2$), 7.0—7.4 (m, 3H, ArH and –C**H**=CH_2), 7.72 (s, 1H, ArH); MS *m/z* 385 (M^++2), 383 (M^+).

2-Bromo-4-[*N*-*t*-butyl-*N*-(*t*-butyldimethylsiloxy)amino]styrene (*o*-4b): Yield 19%; IR (NaCl) 3090 (νC–H(Ar)), 2860—2960 (νC–H(Alkyl)), 1630 cm^{-1} (νC=C); ^{1}H NMR ($CDCl_3$, 270 MHz) δ=−0.12 (s, 6H, Si–CH_3), 0.90 (s, 9H, Si–*t*-butyl), 1.08 (s, 9H, *N*-*t*-butyl), 5.27 (d, 1H, J=11 Hz, –CH=C**H**$_2$), 5.64 (d, 1H, J=17 Hz, –CH=C**H**$_2$), 7.00 (dd, 1H, J=11, 17 Hz, –C**H**=CH_2), 7.12 (d, 1H, J=8 Hz, ArH), 7.40 (d, 1H, J=8 Hz, ArH), 7.45 (s, 1H, ArH); ^{13}C NMR ($CDCl_3$) δ=−4.63, −2.94, 17.92, 25.72, 26.09, 26.13, 61.35, 115.45, 122.25, 124.26, 125.08, 128.99, 133.53, 135.42, 151.93; MS *m/z* 385 (M^++2), 383 (M^+).

Polymerization. Palladium acetate (0.3 mmol), tri-*o*-tolylphosphine (0.6 mmol), and triethylamine were added to a 0.3 M DMF solution of the monomer (10 ml). The solution was then heated at 100 °C for 6—24 h. The mixture was purified by polystyrene gel permeation chromatography and by reprecipitation from THF in methanol twice, to yield polymers as yellowish powders.

Poly[[2-[*N*-*t*-butyl-*N*-(triethylsiloxy)amino]-1,4-phenylene]-vinylene] (*p*-3a): Yield 48%; IR (KBr pellet) 3055—3030 (νC–H-(Ar)), 2879—2959 (νC–H(Alkyl)), 970 cm^{-1} (δ *trans*-HC=CH); ^{1}H NMR ($CDCl_3$, 400 MHz) δ=0.6 (q, 6H, J=8 Hz, Si–C**H**$_2$CH$_3$), 0.8 (t, 9H, J=8 Hz, Si–CH$_2$C**H**$_3$), 1.1 (s, 9H, *N*-*t*-butyl), 6.9—8.1 (m, 5H, ArH and CH=CH). Found: C, 69.5; H, 9.6; N, 4.5; Br, 2.1%. Calcd for $C_{18n}H_{29n+1}BrN_nO_nSi_n$ (n=11): C, 69.5; H, 9.4; N, 4.5; Br, 2.3%.

Poly[[4-[*N*-*t*-butyl-*N*-(*t*-butyldimethylsiloxy)amino]-1,2-phenylene]vinylene] (*o*-3b): Yield 60%; IR (KBr pellet) 2860 (νC–H(Alkyl)), 960 cm^{-1} (δ *trans*-HC=CH); ^{1}H NMR ($CDCl_3$, 500 MHz) δ=−0.1 (s, 6H, Si–CH_3), 0.8 (s, 9H, Si-*t*-butyl), 1.1 (s, 9H, *N*-*t*-butyl), 6.9—7.5 (m, 5H, ArH and CH=CH); ^{13}C NMR ($CDCl_3$) δ=−4.59, 17.94, 26.20, 61.06, 122.76, 124.7—125.5, 127.5, 127.8—128.8, 132.4, 135.56, 143—144, 150.83. Found: C, 70.0; H, 9.4; N, 4.4; Br, 1.6%. Calcd for $C_{18n}H_{29n+1}BrN_nO_nSi_n$ (n=16): C, 70.1; H, 9.5; N, 4.5; Br, 1.6%.

Oligomerization. Palladium acetate (6.7 mg, 0.030 mmol), *o*-tolylphosphine (18 mg, 0.060 mmol), and triethylamine (1.1 g) were added to a 5 ml DMF solution of *o*-**4b** (1.2 g, 3.0 mmol) and styrene (0.31 g, 3.0 mmol) under a nitrogen atmosphere; the solution was then stirred for 3 h at 100 °C. On the other hand, palladium acetate (6.7 mg, 0.030 mmol), *o*-tolylphosphine (18 mg, 0.060 mmol), and triethylamine (1.1 g) were added to a 5 ml DMF solution of *o*-**4b** (1.2 g, 3.0 mmol) and bromobenzene (0.47 g, 3.0

mmol) under a nitrogen atmosphere; the solution was stirred for 3 h at 100 °C. After the Heck coupling reaction traced by TLC, the two reaction mixtures were combined using a cannula, and then stirred for 14 h at 100 °C. The reaction mixture was evaporated, extracted with chloroform, and washed with 10% aqueous hydrochloric acid. After drying over magnesium sulfate, the solution was evaporated and purified by column chromatography on silica gel (chloroform/hexane) followed by separation with HPLC.

1,2-Distyryl-4-[*N*-*t*-butyl-*N*-(*t*-butyldimethylsiloxy)amino]-benzene (7a): Yield 5%; IR (NaCl) 3026 (νC–H(Ar)), 2857—2957 (νC–H(Alkyl)), 959 cm^{-1} (δ *trans*-HC=CH); ^{1}H NMR ($CDCl_3$, 270 MHz) δ = −0.1 (m, 6H, Si–CH_3), 0.9 (s, 9H, Si–*t*-butyl), 1.1 (s, 9H, *N*-*t*-butyl), 6.9—7.5 (m, 17H, ArH and HC=CH); ^{13}C NMR ($CDCl_3$) δ = −4.59, 17.36, 26.16, 61.10, 122.95, 125.50, 126.59, 126.89, 127.67, 128.70, 130.26, 131.00, 136.69, 137.77, 150.82; MS *m/z* 485 (M^++2), 484 (M^++1), 483 (M^+).

2,2′-Distyryl-4,5′-bis[*N*-*t*-butyl-*N*-(*t*-butyl-dimethylsiloxy)-amino]stilbene (8a): Yield 3%; IR (NaCl) 3028 (νC–H-(Ar)), 2857 (νC–H(Alkyl)), 960 cm^{-1} (δ *trans*-HC=CH); ^{1}H NMR ($CDCl_3$, 270 MHz) δ = −0.16 (s, 12H, Si–CH_3), 0.86, 0.79 (s, 18H, Si–*t*-butyl), 1.06, 1.04 (s, 18H, *N*-*t*-butyl), 6.8—7.4 (m, 22H, ArH and HC=CH); ^{13}C NMR ($CDCl_3$) δ = −4.62, 17.97, 26.17, 61.06, 107.93, 122.97, 124.74, 125.43, 125.61, 126.38, 126.51, 126.70, 126.86, 127.42, 127.58, 128.12, 128.28, 128.59, 128.63, 128.73, 130.24, 131.11, 132.44, 132.56, 135.13, 135.56, 137.47, 137.75, 150.76; MS *m/z* 787 (M^++1), 786 (M^+).

3′-Bromo-2-methylstilbene. After palladium acetate (0.18 g, 0.80 mmol) and triethylamine (20 g, 0.20 mol) were added to a 60 ml acetonitrile solution of 3-bromostyrene (7.4 g, 40 mmol) and 2-iodotoluene (8.8 g, 40 mmol) under a nitrogen atmosphere, the mixture solution was stirred for 12 h at 80 °C. The solution was evaporated, washed with 10% aqueous hydrochloric acid, and extracted with ether. After drying over anhydrous sodium sulfate, the ether solution was evaporated and developed on a silica-gel column with hexane. Yield 33%; IR (KBr pellet): 959 cm^{-1} (δ*trans*-HC=CH); MS *m/z* 274 (M^++2), 272 (M^+).

2-(3-Bromostyryl)styrene. After 3′-bromo-2-methylstilbene (2.7 g, 10 mmol) was dissolved in 25 ml of tetrachloromethane. *N*-Bromosuccinimide (1.6 g, 10 mmol) and benzoyl peroxide (0.02 g, 0.1 mmol) had been added to the solution, the mixture was refluxed for 3 h. The mixture was then filtered, and the filtrate was evaporated and dissolved in 20 ml of benzene. Triphenylphosphine (2.6 g, 10 mmol) was added to the solution and stirred for 1 h at 70 °C to yield a white precipitate of the phosphonium salt. The mixture was filtered and washed with ether to yield 4.4 g of [[2-(3-bromostyryl)phenyl]methyl]triphenylphosphonium bromide (yield 72%). The phosphonium salt (3.6 g, 7.0 mmol) was suspended in 36 ml of 25% formalin, and 8 ml of 5 M-sodium hydroxide was added dropwise to the mixture over 20 min. The mixture was stirred for 1 h at room temperature and extracted with ether. The extract was washed with water and dried over anhydrous sodium sulfate. The crude products were separated by silica-gel chromatography with hexane/chloroform (1/1) eluent to yield 1.3 g of 2-(3-bromostyryl)styrene. Yield 83%; IR (KBr pellet) 3059, 3026 (νC–H), 1624 (νHC=CH_2), 961 cm^{-1} (δ *trans*-HC=CH); ^{1}H NMR ($CDCl_3$, 60 MHz) δ = 5.3—5.8 (m, 2H, –CH=C**H**$_2$), 6.7—7.6 (m, 11H, ArH, –C**H**=CH_2 and HC=CH); MS *m/z* 286 (M^++2), 284 (M^+).

1-(3-Bromostyryl)-2-(4-bromostyryl)benzene. Palladium acetate (22 mg, 0.10 mmol) and triethylamine (1.0 g, 10 mmol) were added to a 10 ml acetonitrile solution of 2-(3-bromostyryl)-styrene (1.4 g, 5.0 mmol) and 1-bromo-4-iodobenzene (1.4 g, 5.0 mmol) under a nitrogen atmosphere; the solution was then stirred for 12 h at 80 °C. The solution was evaporated, washed with 10% aqueous hydrochloric acid, and extracted with chloroform. After drying over anhydrous sodium sulfate, the chloroform solution was evaporated and developed on a silica-gel column with hexane. Yield 41%; mp 104—106 °C; IR (KBr pellet) 961 cm^{-1} (δ *trans*-HC=CH); ^{1}H NMR ($CDCl_3$, 400 MHz) δ = 6.86—7.65 (m, 16H, ArH); ^{13}C NMR ($CDCl_3$) δ = 121.63, 122.96, 125.25, 126.75, 126.90, 127.13, 127.99, 128.03, 128.16, 129.47, 130.08, 130.24, 130.38, 130.64, 131.88, 135.65, 135.88, 136.33, 139.60; MS *m/z* 442 (M^++4), 440 (M^++2), 438 (M^+). Found: C, 60.2; H, 3.6%. Calcd for $C_{22}H_{16}Br_2$: C, 60.0; H, 3.7%.

1-[3-(*N*-*t*-Butylhydroxyamino)styryl]-2-[4-(*N*-*t*-butylhydroxyamino)styryl]benzene (6b). A butyllithium (4.4 mmol) solution in 2.8 ml of hexane was added to 1-(3-bromostyryl)-2-(4-bromostyryl)benzene (0.88 g, 2.0 mmol) in 35 ml of ether at −70 °C. After the solution was stirred for 5 h at room temperature, a 2-methyl-2-nitrosopropane (1.7 g, 20 mmol) solution in ether was added to the solution at 0 °C, then stirred for 1 h at room temperature. The solution was first washed with aqueous ammonium chloride and then with water. The ether layer was dried over anhydrous sodium sulfate. After evaporation, the crude product was purified by column chromatography on silica gel with chloroform/ethyl acetate (8/1) to give 0.06 g of 1-[3-(*N*-*t*-butylhydroxyamino)styryl]-2-[4-(*N*-*t*-butylhydroxyamino)styryl]benzene as white crystals. Yield 7%; mp 175 °C; IR (KBr pellet) 3239 (νO–H), 2932—2975 (νalkyl), 959 cm^{-1} (δ *trans*-HC=CH); ^{1}H NMR (DMSO-d_3, 500 MHz) δ = 1.10 (s, 18H, *t*-butyl), 7.05—7.70 (m, 16H, ArH and –CH=CH–), 8.33 (s, 1H, OH), 8.35 (s, 1H, OH); ^{13}C NMR (DMSO-d_3) δ = 26.03, 59.30, 59.61, 122.07, 122.99, 123.72, 124.24, 124.64, 125.76, 125.79, 126.23, 126.28, 127.54, 127.67, 127.73, 130.79, 131.13, 132.94, 135.31, 135.71, 136.46, 150.51, 151.07; MS *m/z* 457 (M^++1), 456 (M^+). Found: C, 79.3; H, 8.2; N, 5.8%. Calcd for $C_{30}H_{36}N_2O_2$: C, 78.9; H, 7.9; N, 6.1%.

1-[3-(*N*-*t*-Butylhydroxyamino)styryl]-4-[4-(*N*-*t*-butylhydroxyamino)styryl]benzene (5b). This compound was prepared by the same procedure as that for **6b**. Yield 12%; mp 208 °C; IR (KBr pellet) 3248 (νO–H), 2974 (νalkyl), 961 cm^{-1} (δ *trans*-HC=CH); ^{1}H NMR (DMSO-d_3, 500 MHz) δ = 1.08 (s, 9H, *t*-butyl), 1.09 (s, 9H, *t*-butyl), 7.16—7.60 (m, 16H, ArH and –CH=CH–), 8.32 (s, 2H, OH); ^{13}C NMR (DMSO-d_3) δ = 26.19, 59.44, 59.72, 122.29, 122.48, 123.82, 124.41, 125.71, 126.74, 126.88, 126.97, 127.75, 127.82, 128.25, 128.67, 132.97, 136.28, 136.50, 136.71, 150.53, 151.23; MS *m/z* 457 (M^++1), 456 (M^+). Found: C, 78.4; H, 7.7; N, 5.8%. Calcd for $C_{30}H_{36}N_2O_2$: C, 78.9; H, 7.9; N, 6.1%.

Oxidation. A benzene or toluene solution of the hydroxylamines (0.5—10 mM) was treated with 10-equivalent silver oxide or lead oxide. After filtration, the benzene solution was freeze-dried. THF or a 2-methyltetrahydrofuran solution of the trialkylsiloxy-bearing amines (0.5—10 mM) was treated with tetrabutylammonium fluoride and fresh lead oxide. After filtration, the solution was extracted with benzene and washed with water. The benzene layer was dried over anhydrous sodium sulfate and then freeze-dried.

Spectroscopic Measurement. The ESR spectra were taken on a JEOL JES-2XG ESR spectrometer with 100-kHz field modulation. The spin concentration of each sample was determined by careful integration of the ESR signal standardized with that of a TEMPO (2,2,6,6-tetramethyl-1-piperidinyloxyl) solution.

The IR, NMR, and mass spectra were measured with a JASCO FT/IR-5300, a GE NMR Instruments Omega 500, a JEOL NMR GSX-400, or a JEOL NMR EX-270, and a Shimadzu GC-MS QP-1000 spectrometer, respectively. The molecular weights of the polymers were estimated by GPC (polystyrene gel column, eluent

THF, polystyrene calibration).

Magnetic Measurement. A 2-methyltetrahydrofran solution of polyradical was immediately used after oxidation. Powder samples and samples diluted with diamagnetic polystyrene were prepared as described previously.[18] The solution or powder samples were contained in a diamagnetic capsule. The magnetization and static magnetic susceptibility were measured with a Quantum Design MPMS SQUID magnetometer. The magnetization was measured from 0.5 to 7 T at 2, 2.5, 3, 5, 10 and 15 K. The static magnetic susceptibility was measured from 2 to 300 K in a field of 0.5 T.

This work was partially supported by a Grant-in-Aid for Scientific Research on Priority Area "Molecular Magnetism" Area No. 228/04242104 and for Scientific Research No. 040852 from the Ministry of Education, Science and Culture. We thank for Prof. T. Enoki (Tokyo Institute of Technology) and Dr. M. Mitsuya (Advanced Research Laboratory, Hitachi Ltd.) for the use of their SQUID magnetometers.

References

1) J. S. Millers and A. J. Epstein, "Proceeding of the Symposium on the 4th Int. Conf. Molecule-Based Magnets," *Mol. Cryst. Liq. Cryst.*, **1995**, 271, 272, 273, and 274.

2) H. Iwamura and J. S. Millers, "Proceeding of the Symposium on the Chemistry and Physics of Molecular Based Magnetic Materials," *Mol. Cryst. Liq. Cryst.*, **1993**, 232, 233.

3) H. C. Longuet-Higgins, *J. Chem. Phys.*, **18**, 265 (1950).

4) W. T. Borden and E. R. Davidson, *J. Am. Chem. Soc.*, **99**, 4587 (1977).

5) K. Itoh, *Pure Appl. Chem.*, **50**, 1251 (1978).

6) N. Mataga, *Theoret. Chim. Acta*, **10**, 372 (1968).

7) A. A. Ovchinnikov, *Theoret. Chim. Acta*, **47**, 297 (1978).

8) D. J. Klein, C. J. Nelin, S. Alexander, and F. A. Matsen, *J. Chem. Phys.*, **77**, 3101 (1982).

9) N. N. Tyutyulkov and S. H. Karabunarliev, *Chem. Phys.*, **112**, 293 (1987).

10) K. Yamaguchi, Y. Toyoda, and T. Fueno, *Synth. Met.*, **19**, 81 (1987).

11) P. M. Lahti and A. S. Ichimura, *J. Org. Chem.*, **56**, 3030 (1991).

12) D. A. Dougherty, *Acc. Chem. Res.*, **24**, 88 (1991).

13) H. Iwamura and N. Koga, *Acc. Chem. Res.*, **26**, 346 (1993).

14) A Rajca, *Chem. Rev.*, **94**, 871 (1994).

15) H. Nishide, N. Yoshioka, K. Inagaki, and E. Tsuchida, *Macromolecules*, **21**, 3119 (1988).

16) N. Yoshioka, H. Nishide, T. Kaneko, H. Yoshiki, and E. Tsuchida, *Macromolecules*, **25**, 3838 (1992).

17) H. Nishide, T. Kaneko, N. Yoshioka, H. Akiyama, M. Igarashi, and E. Tsuchida, *Macromolecules*, **26**, 4567 (1993).

18) H. Nishide, T. Kaneko, M. Igarashi, E. Tsuchida, N. Yoshioka, and P. M. Lahti, *Macromolecules*, **27**, 3082 (1994).

19) Y. Miura, Y. Ushitani, K. Inui, Y. Teki, T. Takui, and K. Itoh, *Macromolecules*, **26**, 3698 (1993).

20) J. Veciana, C. Rovira, N. Ventosa, M. I. Crespo, and F. Palacio, *J. Am. Chem. Soc.*, **115**, 57 (1993).

21) A. Rajca and S. Utamapanya, *J. Am. Chem. Soc.*, **115**, 10688 (1993).

22) N. N. Tyutyulkov and I. P. Bangov, *C. R. Acad. Bulg. Sci.*, **27**, 1517 (1974).

23) A. Fujii, T. Ishida, N. Koga, and H. Iwamura, *Macromolecules*, **24**, 1077 (1991).

24) Y. Miura, K. Inui, F. Yamaguchi, M. Inoue, Y. Teki, T. Takui, and K. Itoh, *J. Polym. Sci., Polym. Chem. Ed.*, **30**, 959 (1992).

25) N. Yoshioka, P. M. Lahti, T. Kaneko, Y. Kuzumaki, E. Tsuchida, and H. Nishide, *J. Org. Chem.*, **59**, 4272 (1994).

26) T. Kaneko, S. Toriu, Y. Kuzumaki, H. Nishide, and E. Tsuchida, *Chem. Lett.*, **1994**, 2135.

27) H. Nishide, T. Kaneko, T. Nii, K. Katoh, E. Tsuchida, and K. Yamaguchi, *J. Am. Chem. Soc.*, **117**, 548 (1995).

28) I. Murase, T. Ohnishi, T. Noguchi, and M. Hirooka, *Polym. Commun.*, **25**, 327 (1984).

29) D. R. Gagnon, J. D. Capistran, F. E. Karasz, and R. W. Lenz, *Polym. Bull.*, **12**, 293 (1984).

30) R. N. McDonald and T. W. Campbell, *J. Am. Chem. Soc.*, **82**, 4669 (1960); A. Lapitskii, S. M. Makin, and A. A. Berlin, *Vysokomol. Soedin., Ser. A*, **A9**, 1274 (1967).

31) R. F. Heck, *Org. React.*, **27**, 345 (1982).

32) W. Heitz, W. Brügging, L. Freund, M. Gailberger, A. Greiner, H. Jung, U. Kampschulte, N. Niessner, F. Osan, H. W. Schmidt, and M. Wicker, *Makromol. Chem.*, **189**, 119 (1988).

33) G. Märkl and A. Merz, *Synthesis*, **1973**, 295.

34) A. R. Forrester and S. P. Hepburn, *J. Chem. Soc. C*, **1970**, 1277.

35) T. W. Greene, "Protective Group in Organic Synthesis," John Wiley, New York (1981).

36) G. A. Kossmehl, in "Handbook of Conducting Polymers," ed by T. A. Skotheim, Marcel Dekker, Inc., Basel (1989), Vol. 1, p. 351.

37) T. Kaneko, E. Ito, K. Seki, E. Tsuchida, and H. Nishide, *Polym. J.*, in press.

38) J. Obrzut and F. E. Karasz, *J. Chem. Phys.*, **87**, 2349 (1987).

39) H. Kihara, "Program for Pariser-Parr-Pople SCF MO Calculation with Variable Beta & Gamma Method," Maruzen, Tokyo (1989).

40) P. Tomasello, W. V. Niessen, J. Schirmer, and L. S. Cederbaum, *J. Electron Spectros. Relat. Phenom.*, **40**, 193 (1986).

41) B. G. Zykov, V. V. Martin, and I. A. Grigoryev, *J. Electron Spectrosc. Relat. Phenom.*, **56**, 73 (1991).

42) A. R. Forrester and S. P. Hepburn, *J. Chem. Soc. C*, **1971**, 3322.

43) These spectra involve two small signals between the three-split lines, which is probably ascribed to a partial intermolecular exchange interaction (P. Ferruit, D. Gill, M. P. Klein, H. H. Wang, G. Entine, and M. Calvin, *J. Am. Chem. Soc.*, **92**, 3704 (1970)) between the coplanar distyrylbenzene radicals.

44) H. Nishide, T. Kaneko, S. Toriu, K. Katoh, M. Takahashi, E. Tsuchida, and K. Yamaguchi, *Mol. Cryst. Liq. Cryst.*, **272**, 131 (1995).

45) R. L. Carlin, "Magnetochemistry," Springer-Verlag, Berlin (1986).

46) W. Z. Heisenberg, *Physica, (Amsterdam)*, **49**, 619 (1928).

47) J. H. V. Vleck, "The Theory of Electric and Magnetic Susceptibilities," Oxford University Press, London (1932).

48) B. Bleaney and K. D. Bowers, *Proc. R. Soc. London, Ser. A*, **A214**, 451 (1952).

49) T. Kaneko, S. Toriu, E. Tsuchida, H. Nishide, D. Yamaki, G. Maruta, and K. Yamaguchi, *Chem. Lett.*, **1995**, 421.

50) K. Kambe, *J. Phys. Soc. Jpn.*, **5**, 48 (1950).